AIAA JOURNAL
Vol. 60, No. 8, August 2022

Physics-Based Data-Driven Buffet-Onset Constraint for Aerodynamic Shape Optimization

Jichao Li*
National University of Singapore, Singapore 117575, Republic of Singapore
Sicheng He†
University of Michigan, Ann Arbor, Michigan 48109
Mengqi Zhang‡
National University of Singapore, Singapore 117575, Republic of Singapore
Joaquim R. R. A. Martins§
University of Michigan, Ann Arbor, Michigan 48109
and
Boo Cheong Khoo¶
National University of Singapore, Singapore 117575, Republic of Singapore

https://doi.org/10.2514/1.J061519

Transonic buffet is undesirable because it causes vibration, and constraining buffet is crucial in transonic wing design. However, there is still a lack of accurate and efficient buffet formulation to impose the constraint. This work proposes a physics-based data-driven buffet analysis model generalizable for airfoil and wing shapes. The model is trained with data obtained from two-dimensional airfoils in a physics-based manner to extend it to buffet analyses of three-dimensional wings. Specifically, the model takes the pressure and friction distributions as inputs to discover the key physics (shock waves and flow separation) of transonic buffeting, rather than using shape and flow parameters as the input. High-quality sample airfoils are used and a mixture model of convolutional neural networks is proposed to improve accuracy. The model exhibits a mean absolute error of 0.05 deg in buffet factor prediction of 14,886 unseen testing data. Buffet boundary predictions using the model compare well with the reference results (a lift-curve break method) for various airfoils and wings. Wing shape optimization using the model appropriately considers buffet constraints, leading to an optimized wing with lower drag (by 1.7 counts) than that obtained by the state-of-the-art method. These results demonstrate the effectiveness of the proposed physics-based data-driven buffet analysis approach. The proposed method is a promising alternative to address other complex off-design constraints in aircraft design.

Nomenclature

C_D	=	drag coefficient
C_f	=	friction coefficient
C_L	=	lift coefficient
C_M	=	pitching-moment coefficient
C_p	=	pressure coefficient
M	=	Mach number
n_{Re}	=	number of Reynolds numbers used in section selection
n_{sec}	=	number of wing sections
n_{shape}	=	number of shape design variables
n_{wing}	=	number of wing samples used in section selection
Re	=	Reynolds number
α	=	angle of attack
β	=	buffet factor
γ	=	twist angle
φ	=	probability density function
χ	=	separation metric

I. Introduction

TRANSONIC buffet is caused by shock-induced flow separation [1,2], which is usually located at the foot of shock waves. With an increase of the lift coefficient or Mach number, the strength of shock waves increases, and buffet gradually develops. The condition at which buffet first occurs is called buffet onset. Buffet is undesirable because it affects aircraft control ability, passenger comfort, and even structural integrity. For commercial aircraft, to leave a safety margin for aircraft to maneuver and handle turbulence disturbances, it is stipulated (e.g., by the Federal Aviation Administration and the European Union Aviation Safety Agency) that at least a 30% lift margin from the cruise operating condition to the buffet-onset boundary be maintained. Thus, it is necessary to quantify buffet onset and apply corresponding constraints in aerodynamic shape optimization.

A direct analysis of buffet may involve high-fidelity time-accurate simulations using computational fluid dynamics (CFD), such as unsteady Reynolds-averaged Navier–Stokes (URANS) [3–5], detached-eddy simulations [6–8], and large-eddy simulations [9,10]. Nevertheless, these methods are too computationally expensive for aircraft shape optimization tasks as simulations may be called for hundreds of times, even for a single-point optimization problem. To reduce the computational cost, researchers have been working on developing alternative approaches to evaluating buffet onset based on steady CFD simulations.

Buffet phenomenon has been explained from the view of global instability [1], and thus, a global linear stability analysis of the steady flow solved by Reynolds-averaged Navier–Stokes (RANS) [11,12] can be used to analyze buffet onset. This linear stability analysis approach is accurate in buffet analysis of the NASA Common Research Model (CRM) [13] wing, where an iterative inner–outer Krylov approach with shift-and-invert spectral transformation and sparse iterative linear solver is used to solve the large-scale eigenvalue problem. Because only one linear equation is solved,

Received 6 December 2021; revision received 28 February 2022; accepted for publication 22 April 2022; published online 13 May 2022.

*Postdoctoral Research Fellow, Department of Mechanical Engineering; cfdljc@gmail.com.
†Postdoctoral Research Fellow, Department of Aerospace Engineering.
‡Assistant Professor, Department of Mechanical Engineering.
§Professor, Department of Aerospace Engineering.
¶Professor, Department of Mechanical Engineering.

the computational cost of this method is much lower than that of the URANS-based method. One potential drawback of this approach is that it is not convenient to implement the adjoint method of the eigenvalue problem. This may affect its applications in high-dimensional aerodynamic shape optimization.

In the industry, there is another heuristic approach to buffet-onset analysis that is just based on the global aerodynamic coefficients, such as the lift-curve break method [14]. This method can be implemented by the $\Delta\alpha = 0.1$ deg formulation, where the buffet-onset point is estimated by the intersection of the lift curve and an auxiliary line defined by offsetting the linear portion of the lift curve to the right by 0.1 deg. With this method, the buffet onset can be evaluated by a few RANS simulations. Although it may be computationally cheaper than the URANS-based method, the cost is still high.

For the aerodynamic design community, it is of great interest to construct low-cost alternatives to impose off-design constraints [15,16]. Several approaches have been developed to constrain buffet via fast postprocessing of CFD solutions. For example, based on experimental studies of the relationship between the shock-wave location and buffet margin, the buffet constraint can be imposed by restricting the shock-wave location to 45 and 55% of the chord in supercritical wing design [17]. Redeker [18] proposed a buffet-onset criterion based on rear separation at 90% of the airfoil chord and validated the effectiveness in buffet boundary analysis of supercritical airfoils. Using the physical mechanism of shock-induced flow separation, which is responsible for the loss of lift and the subsequent lowering of the lift-curve slope, Kenway and Martins [19] proposed a separation metric χ to estimate buffet onset, which can be viewed as the percentage of flow separation area to the wing area. They found that using a cutoff value of $\chi = 4\%$ yields the best agreement with the $\Delta\alpha = 0.1$ deg method and experimental data from the wind-tunnel test. These buffet formulations are suitable for aerodynamic shape optimization because it yields a smooth and computationally cheap constraint. Nevertheless, the accuracy of these approaches is a concern. There seem no studies showing whether the constraint on the shock-wave location is too tight or not. The discrepancies of the Kenway–Martins method could be significant compared with the $\Delta\alpha = 0.1$ deg method. Thus, it is necessary to develop another buffet constraint that can accurately estimate buffet onset and evaluate the transition from prebuffet to postbuffet with a smooth metric.

This paper aims to address the demand by developing a generalizable data-driven formulation of transonic buffet. Data-driven models with deep-learning neural networks are capable of modeling complex functions and have been successfully used in solving various aerospace engineering problems [20,21]. With adequate training data, it is possible to train a deep-learning model that provides fast and accurate buffet analysis despite the complexity of buffet phenomena. Commonly used data-based surrogate models for aerodynamic shape optimization are usually defined to approximate the function between shape parameters and the concerned aerodynamic metrics (such as drag and lift coefficients [22–25]). However, this approach lacks generalization due to unawareness of physics, and the trained models cannot be used when the shape parameter space is changed, for example, from two-dimensional geometries to three-dimensional ones. To develop a buffet constraint formulation that is generalizable for aerodynamic shape optimization of both two-dimensional airfoils and three-dimensional wings, we present a physics-based data-driven model that uses the key physics information of transonic buffet (i.e., the shock wave and flow separation).

The procedure to construct the physics-based data-driven buffet analysis model is detailed as follows. We first train a data-driven buffet analysis model that takes as inputs the pressure and friction-coefficient distribution of two-dimensional airfoil samples. To train the model in a sample-efficient way, it is essential to maintain the geometric validity of the sample shapes [22]. We generate high-quality training airfoils by defining a compact geometric design space [26–28], and the airfoils maintain geometric diversity without introducing abnormalities. Then, benefiting from the physics-based feature, we extend the data-driven model to buffet analysis of three-dimensional wings by developing an automatic wing-section selection algorithm. The accuracy and generalization of this data-driven buffet model are verified with the $\Delta\alpha = 0.1$ deg method in buffet boundary analyses of different airfoils and wings, including the CRM wing [29], the ONERA–The French Aerospace Lab (ONERA) M6 wing [30], and a blended wing–body (BWB) configuration [31,32]. Finally, we demonstrate the performance of this model in aerodynamic shape optimization of the CRM wing with buffet constraints.

The rest of this paper is organized as follows. The physics-based data-driven buffet constraint is described and verified on two-dimensional airfoils in Sec. II. We present its extension to buffet analysis of three-dimensional wings in Sec. III. Then, its performance in wing shape optimization is investigated in Sec. IV. The conclusions are summarized in Sec. V with a discussion on the pros and cons of the proposed model.

II. Physics-Based Data-Driven Buffet Analysis

A. Buffet Analysis with the Lift-Curve Break $\Delta\alpha = 0.1$ Degree Method

Compared with low-fidelity buffet models used in conceptual aircraft design optimization [33], the lift-curve break method coupled with RANS is more reliable [34], and it can evaluate the effect of sectional shape changes in detailed aerodynamic shape optimization. Although RANS cannot reveal the physical dynamics of unsteady oscillations, it is suitable to use RANS in flow simulations before buffet onset. Several studies [19,35] showed that steady RANS predictions were consistent with flight data in the buffet-onset regime. As introduced previously, the $\Delta\alpha = 0.1$ deg method is an implementation of the lift-curve break method [14] by introducing an auxiliary line that offsets the linear portion of the lift curve. The slope of the auxiliary line can be evaluated using the finite difference (FD) method between two small angles of attack, where the lift usually changes linearly. Nevertheless, selecting the two FD angles will introduce ambiguity to the estimated buffet-onset point. We investigate this influence in buffet analysis of the RAE 2822 airfoil with $Re = 5.0 \times 10^6$ at different Mach numbers. The following three pairs of FD angles are used to evaluate the slope of the auxiliary line: $\{-1.0; -0.5$ deg$\}$, $\{-1.0; 0.5$ deg$\}$, and $\{-1.0; 1.5$ deg$\}$. As shown in Fig. 1, different choices lead to different buffet-onset points that are marked as the shaded areas, and this effect is significant at high Mach numbers ($M > 0.75$), where buffet onset occurs at a low angle of attack with an increase in the shock-wave strength. Thus, the lift curve in the high-Mach-number regime becomes nonlinear at small angles of attack. For other airfoils, it can be anticipated that there would be a similar trend despite that the ambiguity effect may differ, and a suitable selection of the FD angles may be case dependent and require a specific investigation of the linear portion of the lift curve.

As stated by Kenway and Martins [19], due to the ambiguity, using the $\Delta\alpha = 0.1$ deg method to construct a buffet constraint would cause the optimizer to exaggerate the buffet onset by manipulating the "linear" portion of the lift curve. To address the issue, Kenway and Martins [19] proposed to constrain buffet onset based on a separation metric χ, which is an approximation of the $\Delta\alpha = 0.1$ deg method but works better in evaluating the change of aerodynamic shape for aerodynamic optimization. This approach makes it much more convenient to impose buffet constraints in CFD-based aerodynamic shape optimization. In the following content, we denote their approach as the Kenway–Martins method. As a state-of-the-art buffet-onset constraint formulation, this method has been implemented in open-source CFD solvers (ADflow [36] and SU2 [37]) for aerodynamic shape optimization.

In the investigation of Kenway and Martins [19], using a 4% cutoff of the separation metric yielded the best agreement with the $\Delta\alpha = 0.1$ deg method. We compare the Kenway–Martins method and the $\Delta\alpha = 0.1$ deg method in the buffet boundary evaluation of different airfoils. The result of the $\Delta\alpha = 0.1$ deg method is provided as a shade due to ambiguity in the linear portion selection, as mentioned previously. As shown in Fig. 2, the Kenway–Martins method gives

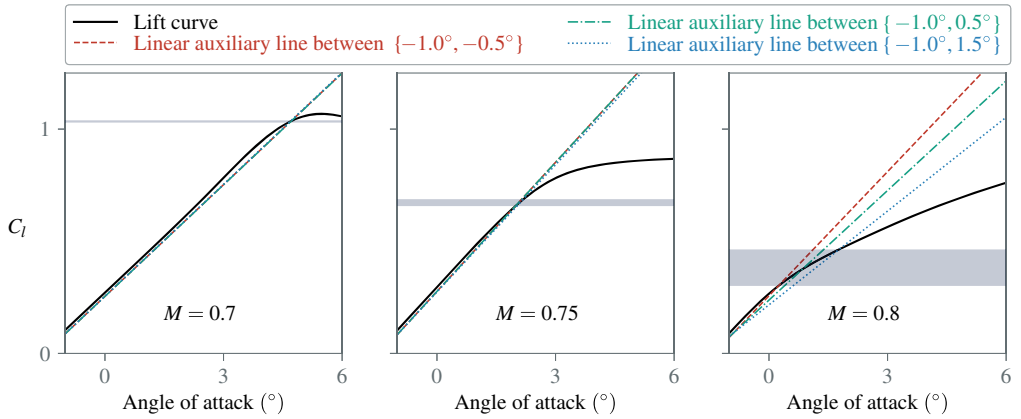

Fig. 1 Selection of the liner auxiliary line introduces ambiguity in buffet-onset analysis for the $\Delta\alpha = 0.1$ deg method.

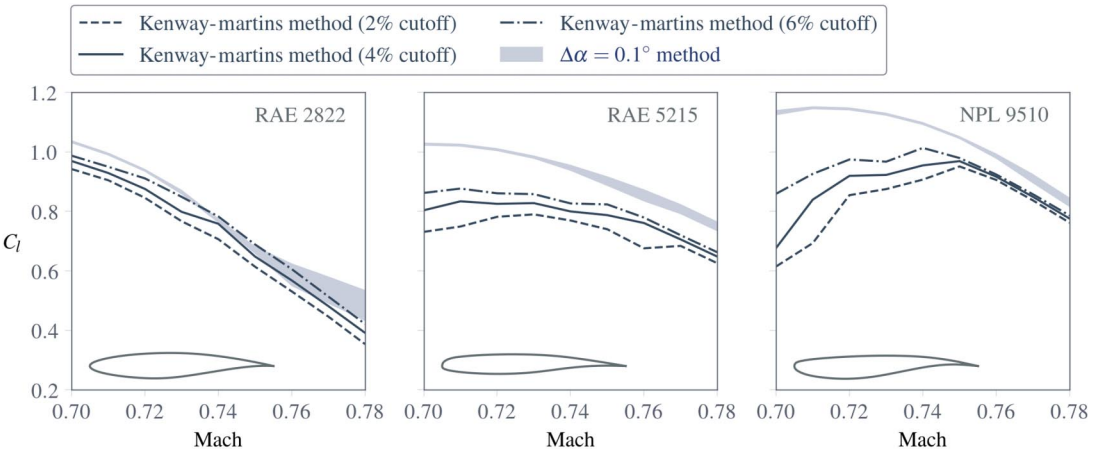

Fig. 2 Buffet boundaries of three airfoils evaluated by the Kenway–Martins formulation [19] and $\Delta\alpha = 0.1$ deg method, respectively.

comparable results at some specific points. Nevertheless, there are notable discrepancies from solutions of the $\Delta\alpha = 0.1$ deg method. It may be because the Kenway–Martins method cannot distinguish the difference between a shock-induced separation and a pure boundary-layer separation, and the constant χ cutoff suitable for a high Mach regime might be too tight at a low Mach regime. (See the buffet-onset boundary drop at low Mach numbers in Fig. 2.) This motivates us to construct an accurate method for buffet analysis that can provide similar results to the $\Delta\alpha = 0.1$ deg method and maintain the advantages of the Kenway–Martins method.

B. Data-Driven Formulation

We construct a data-driven buffet analysis model based on training data of two-dimensional airfoils labeled by the $\Delta\alpha = 0.1$ deg method. The model is formulated in a physics-based manner for extensibility to three-dimensional shape analysis.

1. *Inputs and Output*

Transonic buffet is a coupled effect of shock waves and flow separations. Instead of using parameters of aerodynamic shape and flow conditions as the input, we feed the data-driven model with sectional data of the physical flowfields, that is, the distributions of pressure coefficients C_p and friction coefficients C_f, which reflect shock waves and flow separations, respectively. This physics-based formulation enables analyses of arbitrary airfoils or wing sectional shapes. Flow condition parameters, such as Mach number M, angle of attack α, and Reynolds number Re, are not explicitly used as the inputs for ease of extension to buffet analysis of three-dimensional wings.

We use C_p and C_f distributions only on the upper surface as the inputs. Although there is a type of buffet where shock oscillations are reported on both the upper and lower surfaces at zero angle of attack [38,39], more commonly, the buffeting phenomenon for aircraft shows up at a positive angle of attack with flow separations mainly on the upper surface [40,41]. Thus, for aerodynamic shape design optimization of aircraft, using data on the upper surface is sufficient, and this choice is beneficial for computation reduction in training data-driven models. We also investigated using data of both surfaces to train the model but observed insignificant improvement in prediction accuracy. We format each distribution by 126 points from the trailing edge to the leading edge using scaled points as follows:

$$x_j = 0.5c\left(\cos\left(\frac{j\pi}{125}\right) + 1\right), \qquad j = 0, 1, \ldots, 125 \tag{1}$$

where c is the length of the airfoil or wing section. Using the distribution of the wall Mach number rather than the pressure coefficient would exclude the influence of Mach number M and might be worth investigating.

For a given shape at a fixed Mach number, transonic buffet gradually develops with the increase of the angle of attack. To be used as an effective constraint in aerodynamic shape optimization, the data-driven model should predict the buffet-onset point and the distance of the current state from buffet onset, that is, modeling the buffet strength. To this end, we define a buffet factor β as the output of the data-driven model, which is the difference between the current angle of attack α and the buffet-onset angle of attack $\alpha_{\text{buffet-onset}}$:

$$\beta = \alpha - \alpha_{\text{buffet-onset}} \tag{2}$$

We compute the buffet-onset angle of attack using the $\Delta\alpha = 0.1$ deg method in this work. The lift curve with $\alpha \in [0; 7$ deg$]$ is solved

by RANS with a 0.5 deg incremental (15 simulations per curve) and then interpolated to be a cubic spline curve to solve the intersection point with an offsetting linear curve. To reduce the impact of ambiguity, we evaluate the linear slope of the lift curve between $\alpha = 0.0$ deg and $\alpha = 0.5$ deg for all training data. The layout of the data-driven model with the inputs and the output will be explained in Sec. II.B.3.

2. *Training Data*

To ensure a good generalization and accuracy, we use plenty of training data covering diverse airfoil shapes and operating conditions (Mach number M, Reynolds number Re, and angle of attack α). A typical issue in generating training samples with shape deformations is the geometric abnormality (shown in Fig. 3). It deteriorates the accuracy of data-based models because their aerodynamic function is much more complicated and distinct from that of realistic shapes [22]. Trying to improve the generalization in these abnormal shapes does not contribute to the analysis of realistic shapes in real-world applications.

This geometric issue has been addressed using the deep-learning-based optimal sampling method [26], which was proposed to improve optimization efficiency in aerodynamic shape design. The sampling method is an optimization process that modifies arbitrary shapes to realistic ones with minimal deformation. The validity of the modified shapes is ensured by enforcing a deep-learning-based geometric constraint that is developed to analyze geometric abnormalities [42]. This geometric validity constraint has been shown to be an effective filter of the geometric space that removes abnormalities without excluding innovative aerodynamic shapes [27]. Any other geometric constraints, such as area and thickness, can be specified in this sampling process. The sampling diversity is ensured by starting from different initial shapes, such as Latin hypercube sampling (LHS) airfoils, or synthetic shapes generated by the generative adversarial network [42]. The optimization problem is solved by pyOptSparse [43,44], and pyGeo [45] is used to evaluate constraints of area and thickness. The Extended Design Structure Matrix (XDSM) diagram [46] of this sampling method is shown in Fig. 4.

In this work, we use the deep-learning-based optimal sampling method [26] to generate high-quality training airfoil shapes. Based on practical needs in transonic shape design, we restrict the airfoil thickness to [6; 15%] of the chord length. We add 10,000 different airfoils step by step to construct and expand the training data set. For each sample airfoil, 15 CFD simulations are performed to evaluate buffet onset. The operating Mach number and Reynolds number are chosen by performing LHS in $M \in [0.69; 0.78]$ and $Re \in [3.0 \times 10^6; 7 \times 10^6]$, where the bounds are defined by referring to typical demands of transonic aircraft. Then, their buffet factors are computed, and all of them are added to the training data set. We use ADflow [36] to run the CFD simulations by solving the RANS equation with the Spalart–Allmaras turbulence model. The approximate Newton–Krylov algorithm implemented in ADflow [47] ensures a fast numerical convergence of RANS even for physically oscillating flows. The mesh size is 251×101, and the first layer thickness is conservatively chosen to be 3×10^{-6} to ensure $y^+ < 1.0$ at all investigated conditions. The analysis results of some sampling airfoils are shown in Fig. 5. The lift curve is evaluated at the sampled operating condition, and the background contours show the pressure coefficients at buffet onset (evaluated by the $\Delta\alpha = 0.1$ deg method). The top-left curves are distributions of pressure coefficients (in black) and friction coefficients (in purple) on the upper surface of airfoils at $\alpha = 1.0$ deg, and the bottom-right ones are those at $\alpha = 6.0$ deg. A total of 150,000 RANS simulations are performed. Because a small percentage of these simulations did not converge, we obtained 148,860 pairs of training data.

3. *Mixture of Convolutional Neural Networks*

Because of its strong modeling capability, convolutional neural network (CNN) has been used to model many complex nonlinear functions, such as geometric validity [27,42], flowfields [48,49], and aerodynamic coefficients [50,51]. We also use CNN to model the buffet factor in this study. Ideally, one universal model should be able to model different buffet phases (characterized by β), even though there are different types of shock/boundary-layer interactions and excitations with the change of shock-wave strength [40].

In practice, however, we find that one universal CNN model cannot accurately predict the buffet boundary. This may be due to the significant diversity in different buffet phases as we consider a

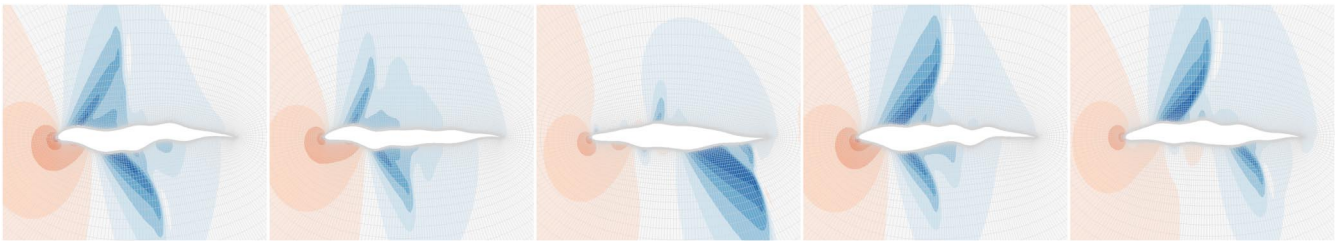

Fig. 3 Geometric abnormality of airfoils that should be avoided in training data-driven models.

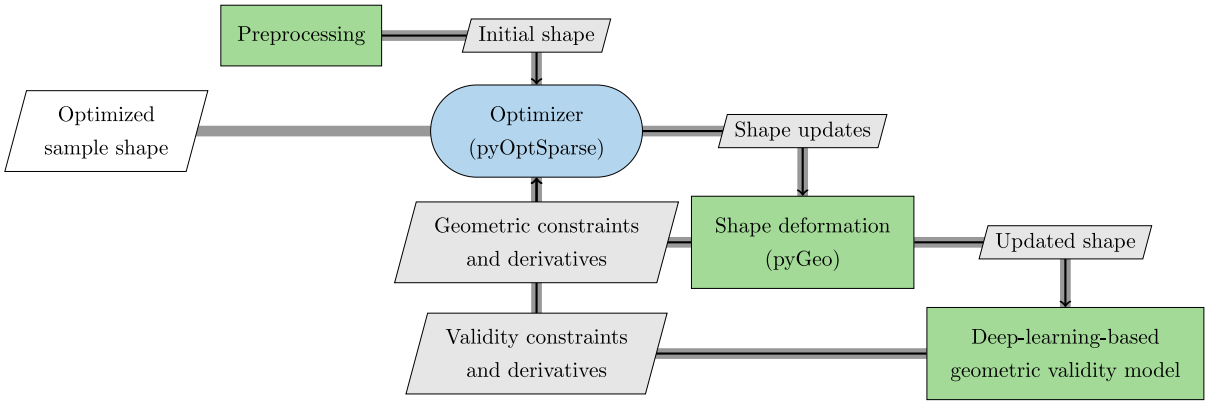

Fig. 4 Deep-learning-based optimal airfoil sampling method.

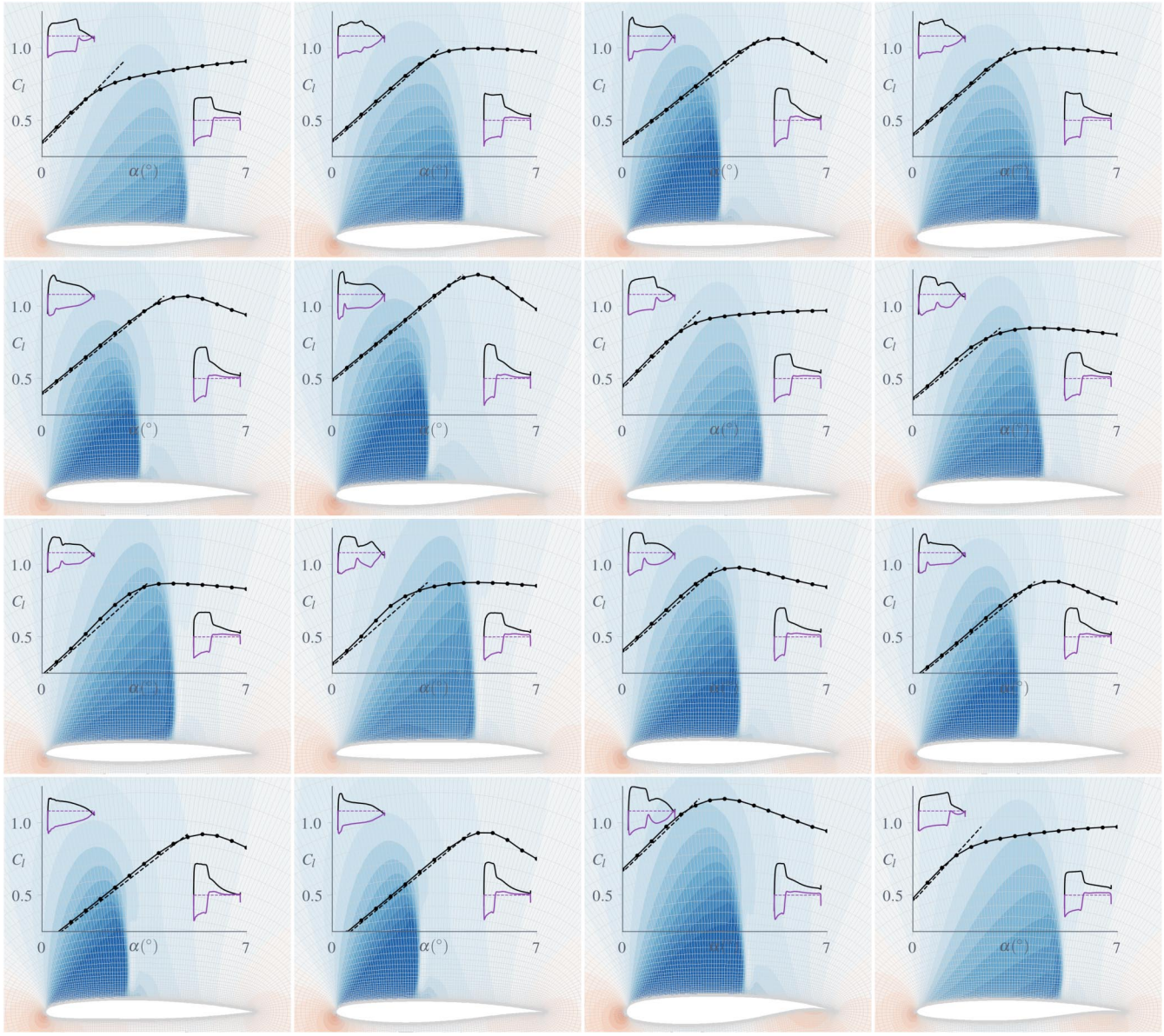

Fig. 5 Deep-learning-based optimal sampling method generates 10,000 sample airfoils evaluated by RANS and labeled by the $\Delta\alpha = 0.1$ deg method.

wide range of angles of attack. With the increase of the angle of attack, the transonic flow may encounter the following three typical phases: weak shock waves at a low angle of attack (prebuffet), strong shock waves inducing flow separations at a moderate angle of attack (buffet onset), and limit cycle oscillations at a large angle of attack (postbuffet). This diversity brings challenges to training one universal prediction model, and similar issues are common in the prediction of aerodynamic coefficients. An effective approach to address it is to use the mixture of experts [52] based on the divide-and-conquer method. For example, Liem et al. [53] showed that using a mixture of kriging models was advantageous in mission analysis of conventional and unconventional aircraft configurations. Similar applications were reported by Li et al. [22] in the construction of a data-based aerodynamic analysis model for arbitrary airfoils.

We propose to improve the accuracy of buffet-onset prediction using a mixture of CNN models. Based on the value of the buffet factor, we divide the training data sets to three domains:

$$\begin{array}{ll} \beta < -0.5 \text{ deg}, & \text{prebuffet} \\ -1.0 \text{ deg} \le \beta \le 1.0 \text{ deg} & \text{buffet onset} \\ \beta > 0.5 \text{ deg}, & \text{postbuffet} \end{array} \tag{3}$$

Then, in addition to the universal CNN that provides an initial buffet analysis, three local CNN models are trained in the divided domains. For a pair of input $\boldsymbol{C}_f$ and $\boldsymbol{C}_p$, the initial buffet factor evaluated by the universal CNN is

$$\beta^{\text{initial}} = \text{CNN}^{\text{initial}}(\boldsymbol{C}_f, \boldsymbol{C}_p) \tag{4}$$

This value is used to evaluate the combination weights of the local CNN models based on three Gaussian distributions, which are defined as $\mathcal{N}(-3.0, 0.7^2)$, $\mathcal{N}(0.0, 0.2^2)$, and $\mathcal{N}(3.0, 0.7^2)$ for prebuffet, buffet onset, and postbuffet, respectively. The probability density functions are denoted as φ^{pre}, φ^{onset}, and φ^{post}. Then, the three local CNN models are combined in a mixture approach to perform buffet analysis in the full domain, where

$$\begin{aligned} \beta^{\text{GMM}} = (&p^{\text{pre}}\text{CNN}^{\text{pre}}(\boldsymbol{C}_f, \boldsymbol{C}_p) + p^{\text{onset}}\text{CNN}^{\text{onset}}(\boldsymbol{C}_f, \boldsymbol{C}_p) \\ &+ p^{\text{post}}\text{CNN}^{\text{post}}(\boldsymbol{C}_f, \boldsymbol{C}_p))/(p^{\text{pre}} + p^{\text{onset}} + p^{\text{post}}) \end{aligned} \tag{5}$$

and

$$p^{\text{pre}} = \varphi^{\text{pre}}(\beta^{\text{initial}})$$
$$p^{\text{onset}} = \varphi^{\text{onset}}(\beta^{\text{initial}})$$
$$p^{\text{post}} = \varphi^{\text{post}}(\beta^{\text{initial}}) \quad (6)$$

The hyperparameters in the four CNN models are determined in a trial-and-error way. We choose a model structure with six convolutional layers, and dropout regularization is used after each layer. The number of filters in each CNN layer is 128. The filter sizes in the first four layers and the last two layers are six and two, respectively. To improve the overall accuracy and stability, downsampling is realized using convolution with a stride $r = 2$ instead of adding a pooling layer. The layout of each CNN model is shown in Fig. 6, and the model is implemented using Keras with TensorFlow as the backend engine.

The process of buffet analysis using the mixture of CNN models is shown in Fig. 7. First, the universal CNN is used to provide an initial buffet analysis (β^{initial}). The second subfigure shows the probability density functions of the Gaussian distributions. The combination weights of local models (the third column in Fig. 7) are evaluated using Eq. (6), and buffet analyses using local models are shown in the fourth column of Fig. 7. Then, the local models are combined to evaluate the buffet factor using Eq. (5), and the analysis result is shown in the last subfigure of Fig. 7.

The accuracy of data-driven models is highly related to the volume of training data. We investigate the effect in this problem by training the CNN models with different numbers of data. As introduced previously, we have performed 150,000 CFD simulations and eventually obtained 148,860 pairs of data except for a few nonconvergence. We choose 10% from these data as the testing data set and randomly select some data from the rest to train the mixture of CNN models. The loss function in CNN models is defined as the mean square error, and 5000 training epochs are used because we find the loss function in the testing data set does not significantly decrease afterward (Fig. 8).

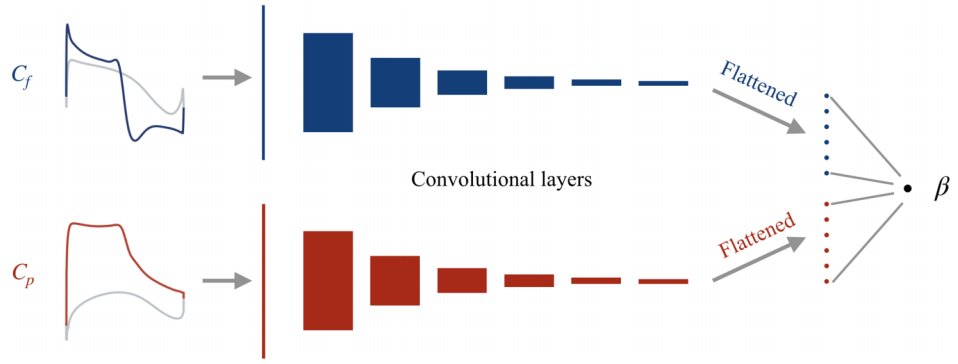

Fig. 6 Layout of CNN models (the four CNN models have the same structure).

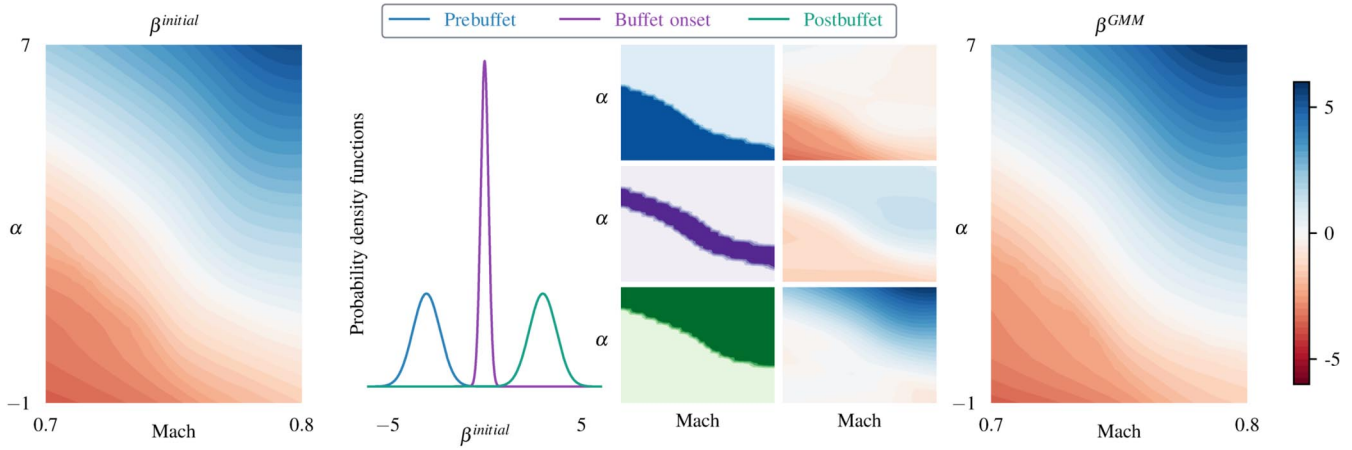

Fig. 7 Mixture of CNN models for buffet analysis.

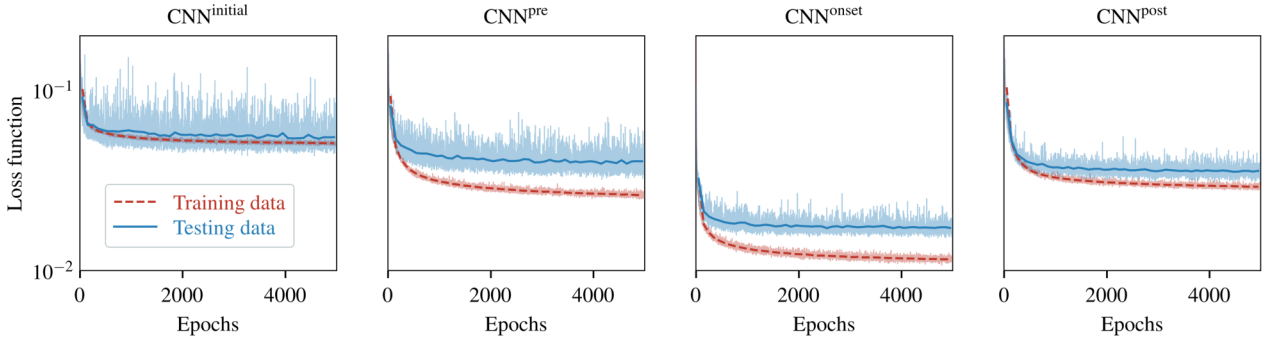

Fig. 8 Loss function reduction histories in the training process of CNN models.

The accuracy of the trained models is evaluated with the testing data set ($n_{\text{test}} = 14{,}886$) using the absolute error $\epsilon = |\beta - \beta^{\text{GMM}}|$, where β and β^{GMM} are the buffet factors obtained by the $\Delta\alpha = 0.1$ deg method and the CNN mixture model, respectively. The errors of the trained models are shown in Fig. 9, where the red line shows the mean absolute error and the gray shade is marked by 25–75% percentiles of the absolute errors. We use the mixture of CNN models trained by 90% of the training data in the following content, and the mean absolute error of the chosen model in the $n_{\text{test}} = 14,886$ testing data is approximately 0.05 deg. The error can be further reduced by adding more training data.

We compare the buffet boundaries of airfoils solved by the data-driven model, the Kenway–Martins method, and the $\Delta\alpha = 0.1$ deg method in Fig. 10. The testing airfoils are three real-world airfoils and three random airfoils generated by the deep-learning-based optimal sampling method introduced in Fig. 4. None of the six airfoils are inside the training data set, and so they are unseen shapes for the data-driven method. Both the data-driven model and the Kenway–Martins method are proposed as approximations of the $\Delta\alpha = 0.1$ deg method. However, compared with the Kenway–Martins formulation, the analysis results of the data-driven method are much closer to those solved by the $\Delta\alpha = 0.1$ deg method. The data-driven method provides a fast and robust approach to buffet analyses of arbitrary airfoils despite some discrepancies.

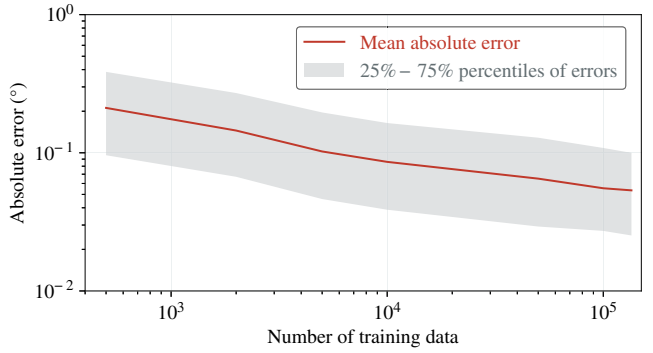

Fig. 9 Errors of the mixture of CNN models trained by different numbers of data.

III. Data-Driven Buffet Analysis of Wings

This work aimed to formulate a robust and efficient buffet-onset constraint for aerodynamic shape design optimization, which is mostly based on three-dimensional shapes, such as wings. To this end, we investigate extending the data-driven method to wing buffet-onset analysis, which is possible with the physics-based feature of the data-driven model.

Our initial assumption is that the wing encounters buffet when buffet onset is detected in any wing sectional airfoils. However, we find this assumption is always too strong, and thus, the predicted buffet-onset angle of attack is smaller than the truth. Although using a conservative criterion is beneficial for safety in aircraft design, an accurate prediction is preferable to maximize the design benefits. So, we relax the assumption as follows: the wing encounters buffet when all of the investigated sectional shapes start buffeting. With this assumption, the buffet factor for wings can be evaluated by the data-driven approach using Algorithm 1.

The choice of investigated wing sections significantly influences the estimated buffet factor. We show this effect in Fig. 11, where the CRM wing is analyzed using RANS ($M = 0.85$, $Re = 5.0 \times 10^6$, and $\alpha = 4.0$ deg). The left and right contours show the pressure and friction coefficients, respectively. The shock wave is shown as

Algorithm 1: Wing buffet factor evaluation using the data-driven method

procedure WingBuffet($\boldsymbol{C}_F$,$\boldsymbol{C}_P$, f) ▷ $\boldsymbol{C}_F$ and $\boldsymbol{C}_P$ are the friction and pressure distributions on the upper surfaces of n_{sec} wing sectional airfoils; f is the data-driven buffet analysis model.
  $\boldsymbol{C}_f = F(\boldsymbol{C}_F)$ ▷ Format the friction description of each section to the 126-point stencil in Eq. (1).
  $\boldsymbol{C}_p = F(\boldsymbol{C}_P)$ ▷ Format the pressure description in the same way.
  for $i = 1; i \le n_{\text{sec}}; i++$ **do** ▷ Traverse the sections.
    $\beta^i = f(\boldsymbol{C}_f^i, \boldsymbol{C}_f^i)$ ▷ Evaluate the buffet factor of each sectional airfoil. $\boldsymbol{C}_f^i$ and $\boldsymbol{C}_p^i$ are the formatted friction and pressure distributions of the i th sectional airfoil.
  end for
  $\beta^{\text{wing}} = \min_{1 \le i \le n_{\text{sec}}} \beta^i$ ▷ Compute the minimal sectional buffet factor.
  return β^{wing} ▷ Return the estimated wing buffet factor.
end procedure

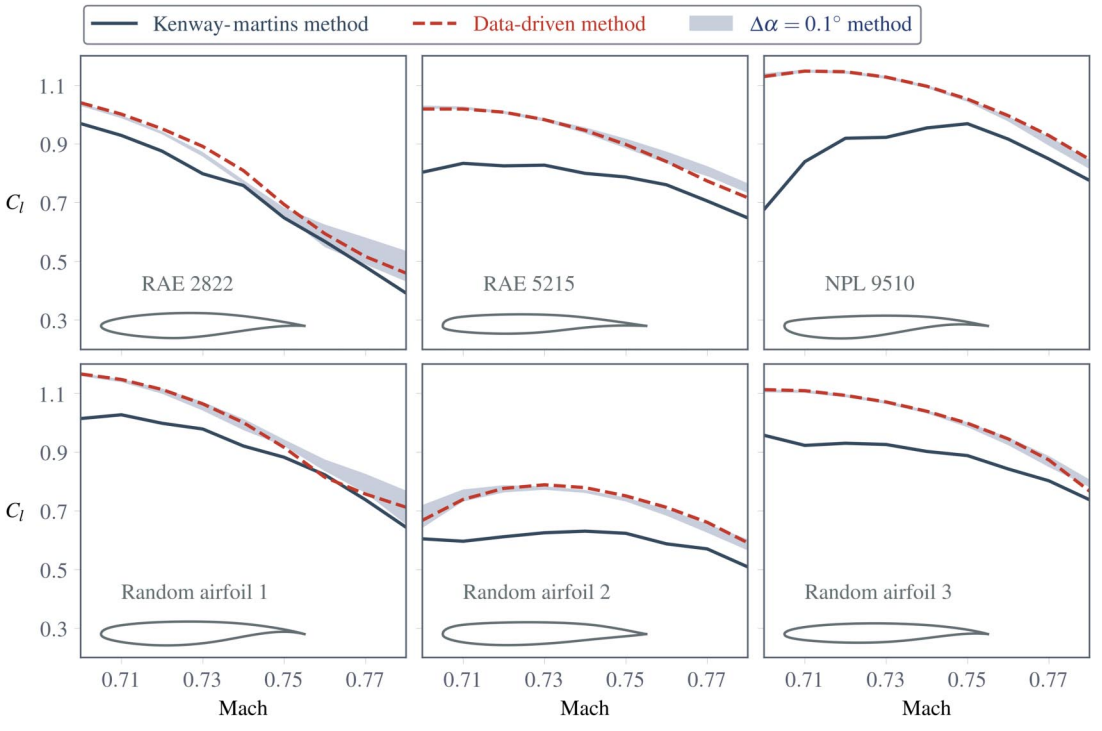

Fig. 10 Buffet boundaries of airfoils solved by the $\Delta\alpha = 0.1$ deg method, the Kenway–Martins formulation [19], and the data-driven method.

the orange domain in the left panel. Seven wing sections (locations indicated by the white slice lines) between the wingtip and the wing root are investigated. Distributions of the pressure coefficients and friction coefficients across the wing sections are shown in the bottom panel, and the data-driven model evaluates the buffet factors of the sectional shapes. The estimated wing buffet factors are different when different subsets of the seven wing sections are used in Algorithm 1, and thus, it is crucial to choose suitable sections for wing buffet analyses. From Fig. 11, we find the flow separations are mostly located outboard of the Yehudi break. Thus, it may be reasonable to choose wing sections from this region for this case. Nevertheless, the appropriate wing sections would be case dependent, and we find that the Mach number has a significant impact.

We propose a data-fitting approach (Algorithm 2) to selecting suitable wing sections for data-driven buffet analysis of wings. In this algorithm, the most suitable wing sections are selected by fitting results of the $\Delta\alpha = 0.1$ deg method. We assume that the selected wing sections are all neighbors with no gaps because the instability origin inducing buffet onset is usually located in a single connected domain [13,34]. The lift distribution could also be investigated in the wing-section selection, which could be a future research direction.

The details of Algorithm 2 are described as follows. First, many sections from the wing root to the wingtip are generated to create a section database from which we will choose subsets for buffet analysis. We perturb the wing shape or the Reynolds number for each Mach number and evaluate the buffet-onset angle of attack using the $\Delta\alpha = 0.1$ deg method. The result is recorded as the reference. Then, we evaluate the buffet-onset angles of attack using Algorithm 1 with different subsets of the database sections and compute the error by comparing with the reference solved in the previous step. Finally, we choose the subset of sections with minimal mean error among all the tests.

As a data-fitting approach, the performance of Algorithm 2 would be impacted by the chosen data (i.e., the number of wing samples n_{wing} and Reynolds numbers n_{Re}). We verify the data-driven method in wing buffet boundary evaluation of the following three wings: the NASA CRM wing [29], the ONERA M6 wing [30], and a BWB configuration defined by Lyu and Martins [31] based on the planform shape of the first-generation Boeing BWB design [32]. For each kind of wing, three wing samples, $n_{\text{wing}} = 3$, are used in Algorithm 2,

Algorithm 2: Wing-section selection

procedure WingSection($\boldsymbol{y}, b, M, Re$) ▷ $\boldsymbol{y}$ is the baseline wing shape, b is the half-wingspan, M is the investigated Mach number, and Re is the investigated Reynolds number.
  $x_i = ib/(n_{\text{sec}} + 1), i = 1, \ldots, n_{\text{sec}}$, ▷ Define n_{sec} evenly distributed sections between the wing root and the wingtip.
  $\{S_1, S_2, \ldots, S_{n_{\text{subset}}}\}$ ▷ Define subsets of n_{sec} wing sections with an assumption that the selected sections in each subset are all neighbors.
  $\{\boldsymbol{y}_1, \boldsymbol{y}_2, \ldots, \boldsymbol{y}_{n_{\text{wing}}}\}$ ▷ Define wing shape database.
  $\{Re_1, Re_2, \ldots, Re_{n_{Re}}\}$ ▷ Define Reynolds-number database.
  $\epsilon^k = 0, k = 1, \ldots, n_{\text{subset}}$ ▷ Initialize the errors.
  for $i = 1; i \le n_{\text{wing}}; i++$ **do** ▷ Traverse the perturbed wing shapes.
    for $j = 1; j \le n_{Re}; j++$ **do** ▷ Traverse the Reynolds numbers.
      $\alpha_{i,j}^{\Delta\alpha} \sim (\boldsymbol{y}_i, Re_j, M)$ ▷ Evaluate the buffet-onset angle of attack using the $\Delta\alpha = 0.1$ deg method.
      for $k = 1; k \le n_{\text{subset}}; k++$ **do** ▷ Traverse the section subsets.
        $\alpha_{i,j}^{k} \sim (\boldsymbol{y}_i, Re_j, M, S_k)$ ▷ Evaluate the buffet-onset angle of attack via Algorithm 1 using sections in subset S_k.
        $\epsilon^k = \epsilon^k + |\alpha_{i,j}^{\Delta\alpha} - \alpha_{i,j}^{k}|/(n_{\text{wing}} n_{Re})$ ▷ Record the error related to the reference.
      end for
    end for
  end for
  $k_{\text{best}} = \text{argmin}_k \epsilon_k$ ▷ Get the subset index with the smallest error.
  return $S_{k_{\text{best}}}$ ▷ Return the selected wing sections.
end procedure

which are generated by perturbing the original wing shape using the modal parameterization method [26]. The Reynolds number is $Re = 5.0 \times 10^6$, $n_{Re} = 1$, in this investigation, and the variation can be included by adding more Reynolds numbers.

In Fig. 12, the left and right panels of each subfigure show the pressure coefficients C_p and friction coefficients C_f along the freestream direction, respectively. Both are the wing upper

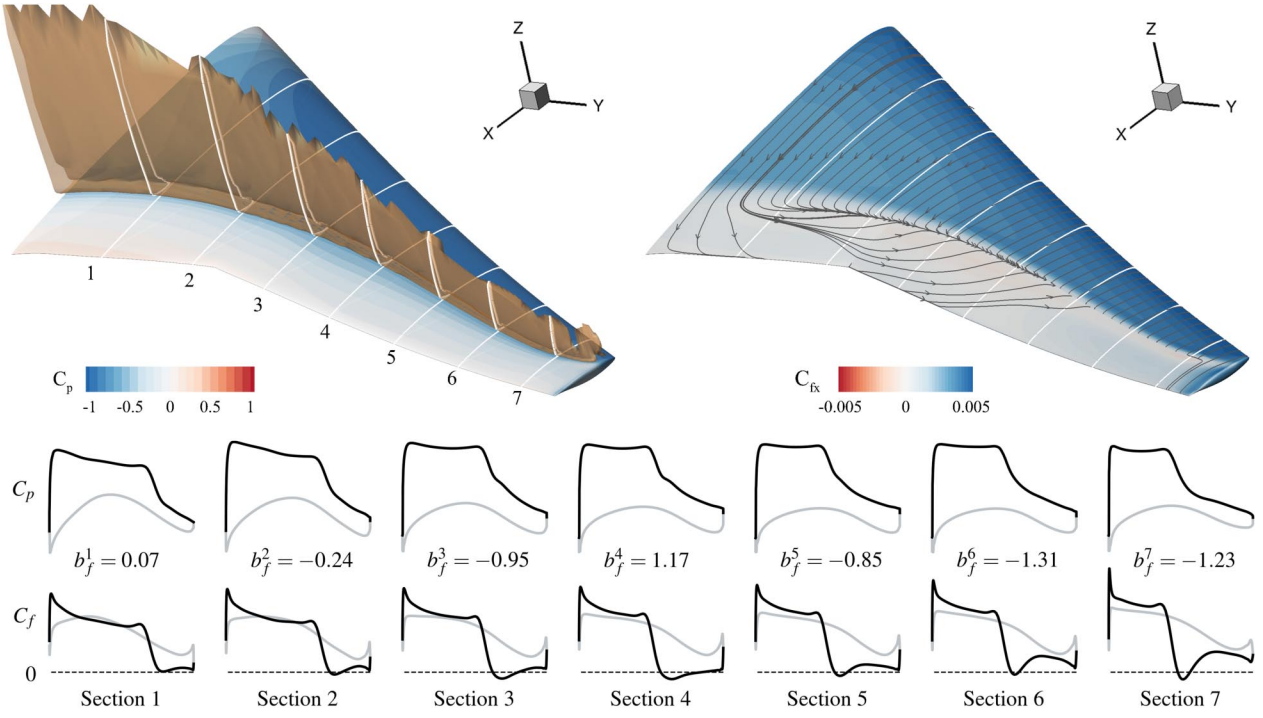

Fig. 11 Buffet analysis of wing sections using the data-driven method.

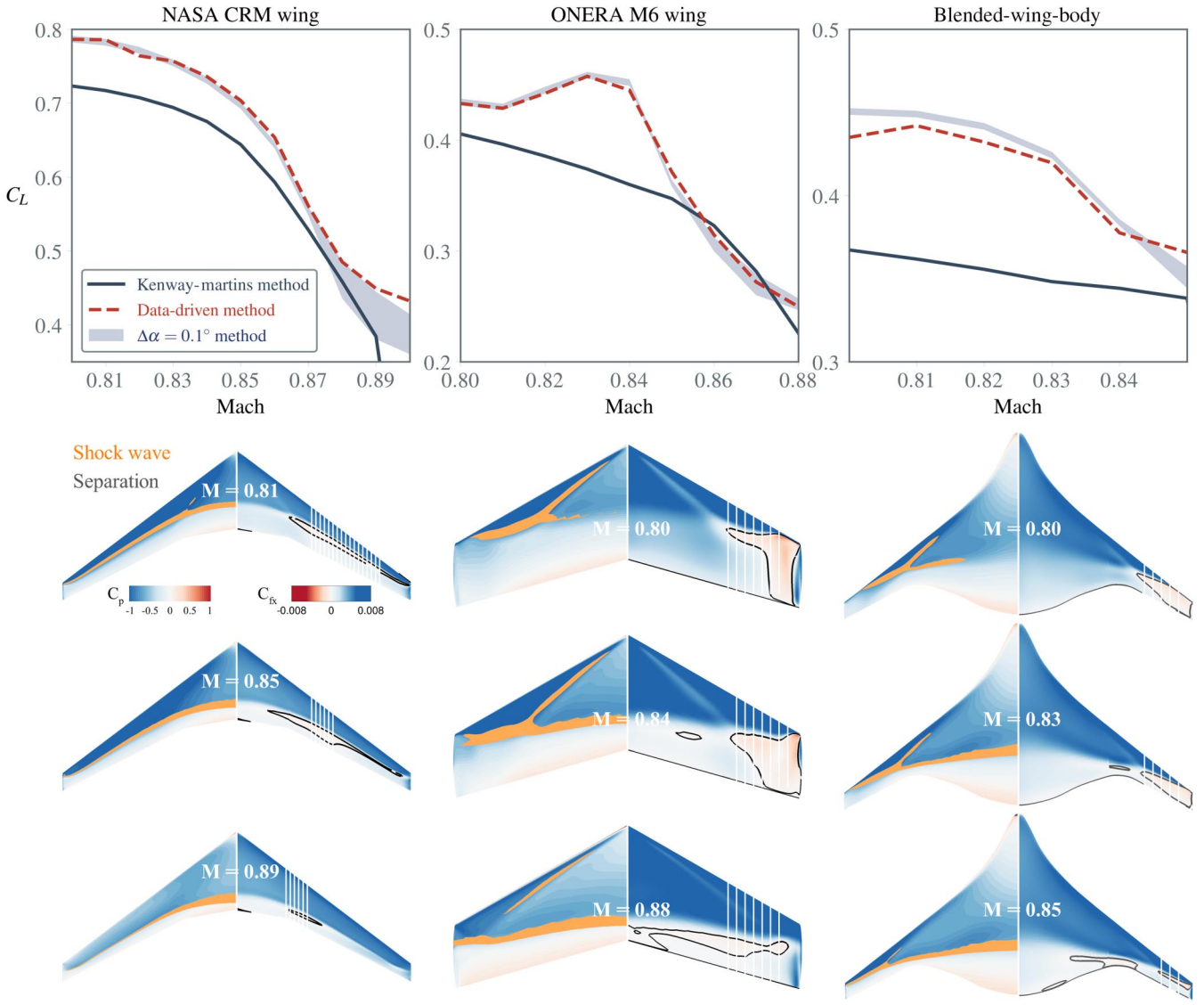

Fig. 12 Verification of the data-driven buffet-onset analysis in different wings.

surface at the buffet-onset angle evaluated by the $\Delta\alpha = 0.1$ deg method. The shock waves are highlighted using orange shades in the left panels, and the recirculation zones (indicating flow separation areas) are shown by black lines in the right panels. The chosen wing sections for data-driven buffet analyses at different Mach numbers are shown as white lines in Fig. 12. In the investigation of Timme [13], the instability origin of transonic buffet was shown to be located at $60 \sim 73\%$ wingspan for the CRM wing at $M = 0.85$ and $Re = 5.0 \times 10^6$. In Fig. 12, the selected wing sections by Algorithm 2 (the CRM wing at $M = 0.85$) are near the instability position, agreeing with the analysis of Timme [13]. The buffet boundaries are evaluated by the following three methods: the Kenway–Martins method, the data-driven method, and the $\Delta\alpha = 0.1$ deg method. With the $\Delta\alpha = 0.1$ deg method as the reference, the data-driven method is more accurate than the Kenway–Martins method. The data-driven model is general enough to evaluate the buffet boundary for different types of three-dimensional wings.

IV. Aerodynamic Shape Optimization

A. Problem Description

We now investigate the effectiveness of the data-driven buffet constraint in wing shape optimization. We minimize the drag of the CRM wing, where the flow condition and aerodynamic constraints are chosen based on the Aerodynamic Design Optimization Discussion Group benchmark case 4, and the geometry is scaled by the mean aerodynamic chord (275.8 in.). The optimization objective is the drag coefficient at the cruise design point ($M = 0.85$ and $C_L = 0.5$), and similar to Kenway and Martins [19], buffet constraints are specified on two off-design points. The first buffet point ($M = 0.85$ and $C_L = 0.65$) is set at the cruise Mach number but with a larger C_L constraint due to the $1.3g$ maneuver. The second buffet point ($M = 0.89$ and $C_L = 0.456$) is 0.04 higher in Mach number, and C_L for this point is adjusted to provide the same lift as that in the cruise point. The Reynolds number at all points is $Re = 5.0 \times 10^6$ for simplification (based on the reference length of the mean aerodynamic chord that is 1.0 in the scaled model). Strict constraints on the wing thickness are specified to obtain practical designs [15]. The optimization problem is detailed in Table 1.

In addition to the optimization case with buffet constraints, a basic study case that only considers the cruise performance is investigated. The considered design points in the two study cases are demonstrated in Table 2 with $n_{\text{point}} = 1$ and $n_{\text{point}} = 3$, respectively. Only the first design point, marked as dots, contributes to the objective function. The others, marked as $\times$, impose buffet constraints.

B. Optimization Framework

An in-house efficient global optimization (EGO) framework, pyAeroEGO [26], is used to solve the wing shape design optimization

Table 1 Wing shape optimization problem statement

	Functions	Description	Quantity
Minimize	C_D	Drag coefficient of the cruise design point	1
With respect to	α^i	Angle of attack	n_{point}
	$\boldsymbol{x}_{\text{shape}}$	Wing shape design variables	n_{shape}
	γ	Wing twists	n_{twist}
		Total design variables	$n_{\text{point}} + n_{\text{shape}} + n_{\text{twist}}$
Subject to	$C_L^i = c^i$	Lift constraints	$i = 1, \ldots, n_{\text{point}}$
	$C_M \geq -0.17$	Moment constraint at the cruise design point	1
	B_{con}^i	Buffet constraints	$i = 2, \ldots, n_{\text{point}}$
	$t \geq t_{\text{initial}}$	Thickness constraints	750
		Total constraints	$750 + 2 \times n_{\text{point}}$

Table 2 Design points of the two optimization cases

Case	Point	M	C_L	$M - C_L$ plot
1	1	0.85	0.5	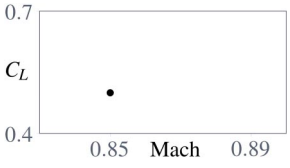
2	1	0.85	0.5	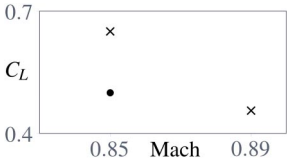
	2	0.85	0.65	
	3	0.89	0.456	

problem. Efficient global optimization has been used in aerodynamic shape optimization for decades. Because of the "curse of dimensionality," this method is mainly applicable to low-dimensionality design problems; it would become too costly for higher-dimensionality problems.

This issue has been addressed by the deep-learning-based modal parameterization method [26] based on geometric filtering [27,42]. The modal parameterization reconstructs the feasible domain of the high-dimensional design space by a low-dimensional modal space, avoiding the dimensionality issue without losing optimization effectiveness. Although the modal parameterization can be implemented independently without other parameterization methods, we implement it on top of the free-form deformation (FFD) method in pyGeo [45] to leverage the convenient built-in geometric functions. Each wing mode involves all the local FFD control points and is treated as an independent global design variable. We use 40 wing modes, $n_{\text{shape}} = 40$, to parameterize the wing shape. As demonstrated in our previous study, optimization with these modes can provide a similar design to that obtained by using 192 FFD control points [26]. Seven twist design variables, $n_{\text{twist}} = 7$, are used to control wing sectional twists. The bounds of the angle of attack and relative angles to the initial wing twists are $[1.0; 4.0 \text{ deg}]$ and $[-1.0; 1.0 \text{ deg}]$, respectively.

Aerodynamic analyses are performed by solving the RANS equations with the Spalart–Allmaras turbulence model using ADflow [36], and the L2 CFD mesh by Lyu et al. [54] is used. The mesh has 507,826 grid nodes, and the height of the first mesh cell off the wall is 1.0×10^{-5}. Aerodynamic shape optimization using this mesh converged to similar results with that using finer meshes [54]. Volume meshes are deformed using an efficient analytic inverse-distance method implemented in IDWarp. In the design of the experiment process, we use 100 initial samples, the number of which is chosen

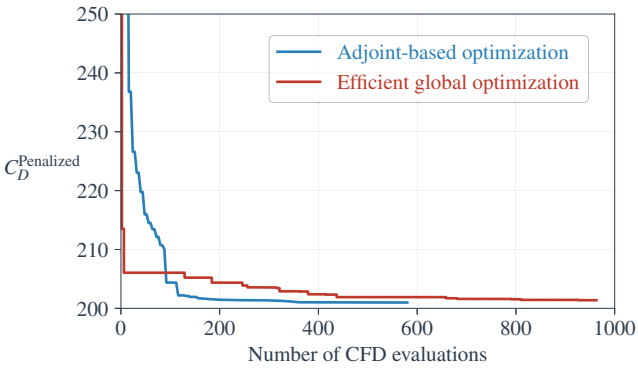

Fig. 14 Comparison of optimization convergence histories shows that EGO with deep-learning-based modal parameterization is comparable to adjoint-based optimization.

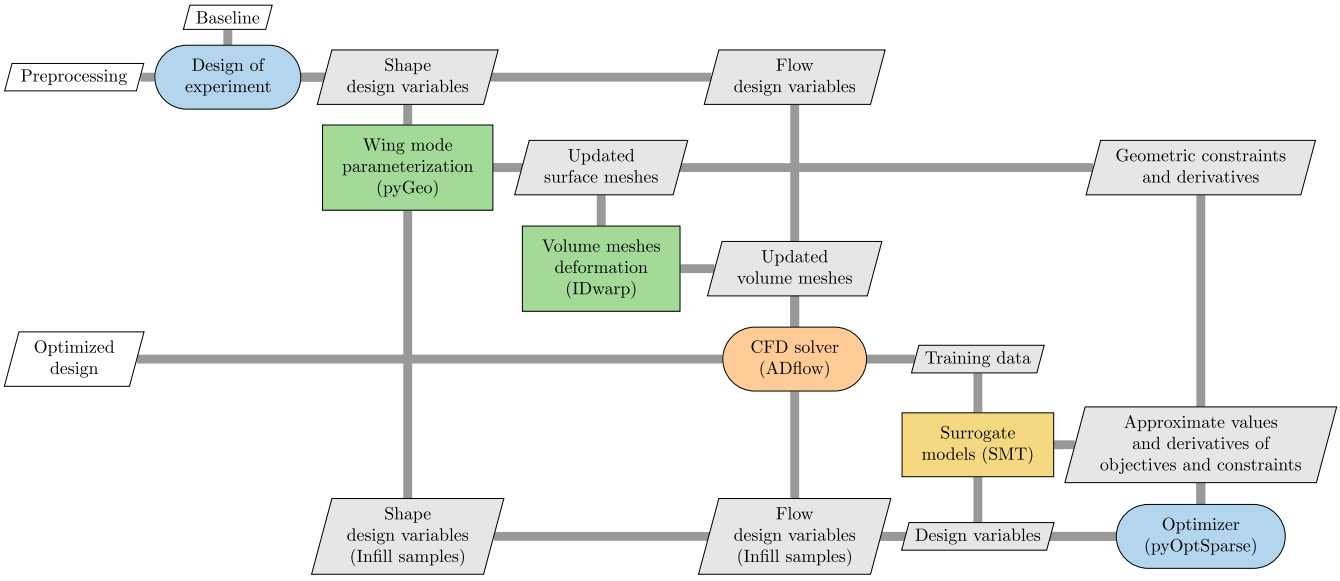

Fig. 13 XDSM diagram of the efficient global optimization framework (pyAeroEGO) with the deep-learning-based modal parameterization.

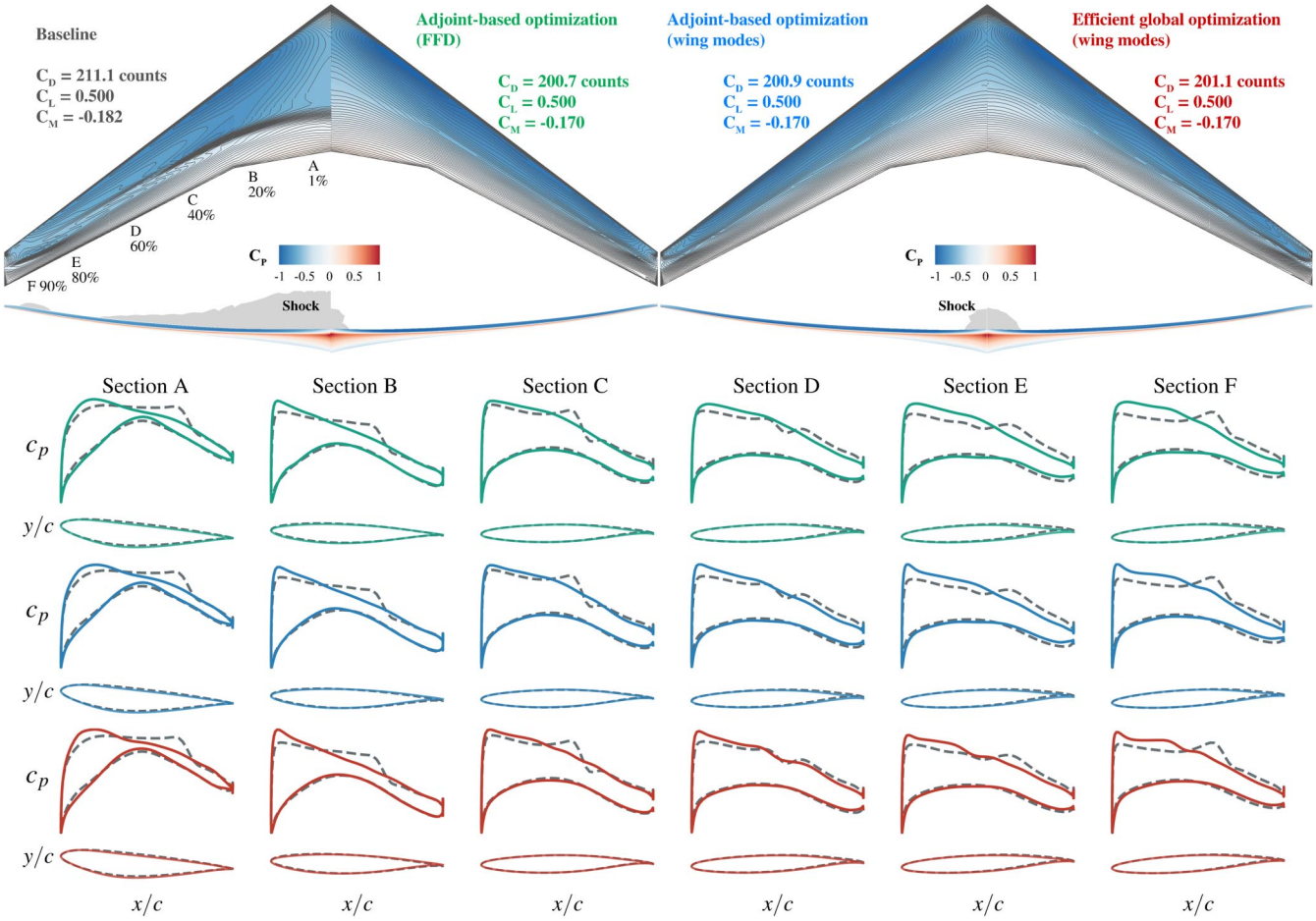

Fig. 15 Comparison of optimized wings shows that deep-learning-based modal parameterization introduces almost no negative effect to optimization effectiveness.

approximately double the number of independent design variables. In EGO, infill samples are added by solving suboptimization problems, minimization of the objective function, and maximization of the expected improvement function, both of which are subject to the required geometric constraints in Table 1. Kriging implemented in the Surrogate Model Toolbox (SMT) is used. The SLSQP algorithm implemented in pyOptSparse [43,44] is used to solve these constrained optimization problems. A multistart strategy is adopted to reduce the possibility of being stuck at local minima ([55]; tip 4.8). In wing shape optimization using modal parameterization, the number of thickness constraints (750) is much higher than the number of shape design variables (40), and this may lead to difficulty in solving the optimization problem. Nevertheless, many thickness constraints are necessary for design practicality (from the structural side) even though a large portion of these constraints might be inactive. Because these constraints are linear, SLSQP can easily handle them with little additional cost. The XDSM diagram of the EGO framework is shown in Fig. 13.

C. Optimization Results

To demonstrate the efficiency and effectiveness of pyAeroEGO in wing shape design optimization, we first investigate case 1 to compare its performance with the adjoint-based optimization conducted using the MACH-Aero framework [56]. Following [26], a metric $C_D^{\text{Penalized}}$ defined as follows is used in measure of the convergence:

$$C_D^{\text{Penalized}} = 10^4 C_D + 10^3 |C_L - 0.5| + 10^3 \max(C_M + 0.17, 0.0) \tag{7}$$

The metric is a weighted sum of the objective function and constraint violations. Thus, a lower value in this metric represents better performance and a lower constraint violation. This metric is only used to show the convergence; we do not use any penalties to deal with constraints in the optimization.

The optimization histories for both pyAeroEGO and MACH-Aero are captured by Eq. (7) and shown in Fig. 14. The adopted EGO framework using modal parameterization is shown to be comparable to the adjoint-based method in optimization effectiveness. (The cost of each adjoint analysis is counted as 0.5 CFD evaluation.) The optimized wings with C_p contours on the wing surface are shown in Fig. 15. Sectional airfoil shapes and the C_p distributions of different optimized wings (in green, blue, and red) are compared with the baseline (in gray). With the modal parameterization, the optimized wings of EGO and adjoint-based optimization almost have the same drag values, and both significantly reduce the areas with shock waves on the wing surface. We also provide the optimized result using the adjoint-based method with 192 FFD control points. We find that reducing the 192-D space to a 40-D modal space only increases the drag count by 0.2 in the solution. This investigation shows that the modal parameterization avoids the curse of dimensionality in wing shape design optimization and has little negative effect on optimization effectiveness. This enables the efficient global aerodynamic shape optimization of wings.

With the optimization effectiveness demonstration in the previous case study, we now apply the EGO framework to case 2. We perform two optimizations with the buffet constraints imposed by the data-driven method ($\beta^{\text{GMM}} \leq 0.0$) and the Kenway–Martins method ($\chi \leq 4\%$), respectively. In the optimization, the wing sections used to evaluate the data-driven buffet factor are shown in Fig. 12, and the Kenway–Martins buffet constraint has already been implemented in ADflow [19,36]. The optimized results are shown in Fig. 16, where the buffet boundaries of the optimized wings are computed using the $\Delta\alpha = 0.1$ deg method. As explained previously, the solved buffet-onset points may vary due to different selections of linear portions of lift curves, and so the boundaries are shown as shades in Fig. 16. The

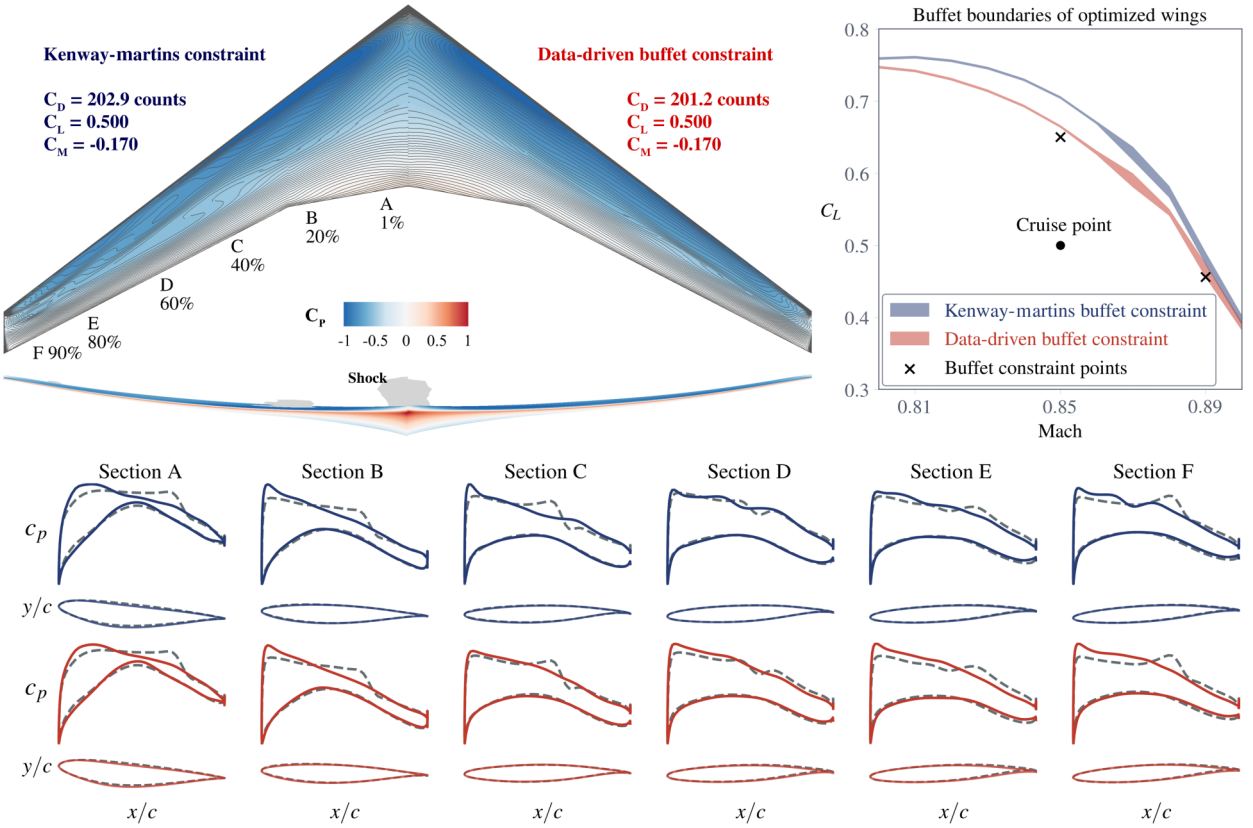

Fig. 16 Wing shape optimization results show that the data-driven method is more effective to impose buffet-onset constraints.

data-driven method appropriately imposes the buffet constraints, and the boundary of the optimized wing almost crosses the two buffet points. However, the Kenway–Martins method is conservative, leading to a wing with a higher buffet boundary than required. The influence of this overstatement is clearly negative: larger cruise drag and more complex shock waves on the wing surface. This negative effect can be anticipated from the comparison in Figs. 10 and 12, where the buffet boundary given by the Kenway–Martins method is usually lower than the reference evaluated by the $\Delta\alpha = 0.1$ deg method. As an accurate alternative of the $\Delta\alpha = 0.1$ deg method, the presented data-driven model provides an efficient way to impose buffet-onset constraints in wing shape design optimization.

V. Conclusions

This work presents a generalizable data-driven approach to imposing buffet-onset constraints in aerodynamic shape optimization. The data-driven model is formulated in a physics-based manner and fed by the pressure- and friction-coefficient distributions that capture the key physics of transonic buffet (i.e., shock wave and flow separation). The output of the data-driven model is the "buffet factor" β, which is defined to quantify the distance from the buffet-onset point. A mixture of CNN models that can handle different phases of buffeting development was developed. Ten thousand high-quality sample airfoils are used to train the mixture of CNN models. Each airfoil is analyzed by performing RANS at 15 angles of attack in [0; 7 deg] to evaluate the buffet factors using the $\Delta\alpha = 0.1$ deg method. An automatic wing section selection algorithm is proposed to extend the data-driven model trained with two-dimensional airfoils to buffet analysis of three-dimensional wings. The verification results show that the model is accurate compared with the reference (i.e., the $\Delta\alpha = 0.1$ deg method) in buffet boundary analysis of airfoils and wings. Wing shape optimization results show that the data-driven buffet constraint is more reliable than the Kenway–Martins method (a state-of-the-art approximation of the $\Delta\alpha = 0.1$ deg method for aerodynamic shape optimization) and improves the cruise performance by exactly satisfying the demands on the buffet boundary.

The accuracy of the proposed model benefits from the high quality of training data with no geometric abnormalities. The good generalization comes from the physics-based feature of the data-driven model. Instead of fitting a function between the shape/flow parameters and the buffet metric, the authors seek to construct the physical relationship between shock separation and buffet onset. Thus, once built, this generalizable relationship applies to various aerodynamic shapes, Mach numbers, and Reynolds numbers. This enables the authors to extend the model trained by two-dimensional airfoils to the buffet analysis of various three-dimensional wings.

One limitation of this work is that the training data are labeled by the $\Delta\alpha = 0.1$ deg method. This method is not accurate even though it is accepted in the industry. Identifying the lift-curve slope introduces ambiguity to the $\Delta\alpha = 0.1$ deg method. This ambiguity results in a noisy buffet function to be modeled, which is harmful to accuracy. Using high-fidelity models in buffet analysis, such as large-eddy simulations, would be more accurate. Future work using high-fidelity models to label the training data would be desirable.

Acknowledgments

The authors acknowledge the Tier 2 grant from the Ministry of Education, Singapore (R-265-000-661-112). The computational resources of the National Supercomputing Centre Singapore (https://www.nscc.sg) are acknowledged.

References

[1] Crouch, J. D., Garbaruk, A., Magidov, D., and Travin, A., "Origin of Transonic Buffet on Aerofoils," *Journal of Fluid Mechanics*, Vol. 628, June 2009, pp. 357–369. https://doi.org/10.1017/S0022112009006673

[2] Plante, F., Dandois, J., Beneddine, S., Laurendeau, É., and Sipp, D., "Link Between Subsonic Stall and Transonic Buffet on Swept and Unswept Wings: From Global Stability Analysis to Nonlinear Dynamics," *Journal of Fluid Mechanics*, Vol. 908, Feb. 2021, p. A16. https://doi.org/10.1017/jfm.2020.848

[3] Thiery, M., and Coustols, E., "URANS Computations of Shock-Induced Oscillations over 2D Rigid Airfoils: Influence of Test Section Geometry,"

Flow, Turbulence and Combustion, Vol. 74, No. 4, 2005, pp. 331–354. https://doi.org/10.1007/s10494-005-0557-z

[4] Gao, C., Zhang, W., Li, X., Liu, Y., Quan, J., Ye, Z., and Jiang, Y., "Mechanism of Frequency Lock-In in Transonic Buffeting Flow," *Journal of Fluid Mechanics*, Vol. 818, May 2017, pp. 528–561. https://doi.org/10.1017/jfm.2017.120

[5] Xu, Z., Saleh, J. H., and Yang, V., "Optimization of Supercritical Airfoil Design with Buffet Effect," *AIAA Journal*, Vol. 57, No. 10, 2019, pp. 4343–4353. https://doi.org/10.2514/1.J057573

[6] Deck, S., "Numerical Simulation of Transonic Buffet over a Supercritical Airfoil," *AIAA Journal*, Vol. 43, No. 7, 2005, pp. 1556–1566. https://doi.org/10.2514/1.9885

[7] Grossi, F., Braza, M., and Hoarau, Y., "Prediction of Transonic Buffet by Delayed Detached-Eddy Simulation," *AIAA Journal*, Vol. 52, No. 10, 2014, pp. 2300–2312. https://doi.org/10.2514/1.J052873

[8] Plante, F., Dandois, J., and Laurendeau, É., "ZDES and URANS Simulations of 3D Transonic Buffet over Infinite Swept Wings," *Progress in Hybrid RANS-LES Modelling*, Springer, Cham, 2019, pp. 259–269. https://doi.org/10.1007/978-3-030-27607-2_21

[9] Garnier, E., and Deck, S., *Direct and Large-Eddy Simulation VII: Proceedings of the Seventh International ERCOFTAC Workshop on Direct and Large-Eddy Simulation*, Springer, Dordrecht, The Netherlands, 2010, pp. 549–554. https://doi.org/10.1007/978-90-481-3652-0_81

[10] Dandois, J., Mary, I., and Brion, V., "Large-Eddy Simulation of Laminar Transonic Buffet," *Journal of Fluid Mechanics*, Vol. 850, Sept. 2018, pp. 156–178. https://doi.org/10.1017/jfm.2018.470

[11] Crouch, J. D., Garbaruk, A., and Magidov, D., "Predicting the Onset of Flow Unsteadiness Based on Global Instability," *Journal of Computational Physics*, Vol. 224, No. 2, 2007, pp. 924–940. https://doi.org/10.1016/j.jcp.2006.10.035

[12] Iovnovich, M., and Raveh, D. E., "Reynolds-Averaged Navier–Stokes Study of the Shock-Buffet Instability Mechanism," *AIAA Journal*, Vol. 50, No. 4, 2012, pp. 880–890. https://doi.org/10.2514/1.J051329

[13] Timme, S., "Global Instability of Wing Shock-Buffet Onset," *Journal of Fluid Mechanics*, Vol. 885, Feb. 2020, p. A37. https://doi.org/10.1017/jfm.2019.1001

[14] Obert, E., *Aerodynamic Design of Transport Aircraft*, IOS Press, Delft, The Netherlands, 2009.

[15] Li, J., He, S., and Martins, J. R. R. A., "Data-Driven Constraint Approach to Ensure Low-Speed Performance in Transonic Aerodynamic Shape Optimization," *Aerospace Science and Technology*, Vol. 92, Sept. 2019, pp. 536–550. https://doi.org/10.1016/j.ast.2019.06.008

[16] Li, R., Zhang, Y., and Chen, H., "Pressure Distribution Feature-Oriented Sampling for Statistical Analysis of Supercritical Airfoil Aerodynamics," *Chinese Journal of Aeronautics*, Vol. 35, No. 4, 2022, pp. 134–147. https://doi.org/10.1016/j.cja.2021.10.028

[17] Zhao, T., Zhang, Y., Chen, H., Chen, Y., and Zhang, M., "Supercritical Wing Design Based on Airfoil Optimization and 2.75D Transformation," *Aerospace Science and Technology*, Vol. 56, Sept. 2016, pp. 168–182. https://doi.org/10.1016/j.ast.2016.07.010

[18] Redeker, G., "Calculation of Buffet Onset for Supercritical Airfoils," *Symposium Transsonicum II*, Springer, Berlin/Heidelberg, 1976, pp. 66–74. https://doi.org/10.1007/978-3-642-81005-3_6

[19] Kenway, G. K. W., and Martins, J. R. R. A., "Buffet-Onset Constraint Formulation for Aerodynamic Shape Optimization," *AIAA Journal*, Vol. 55, No. 6, 2017, pp. 1930–1947. https://doi.org/10.2514/1.J055172

[20] Brunton, S. L., Kutz, J. N., Manohar, K., Aravkin, A. Y., Morgansen, K., Klemisch, J., Goebel, N., Buttrick, J., Poskin, J., Blom-Schieber, A. W., Hogan, T., and McDonald, D., "Data-Driven Aerospace Engineering: Reframing the Industry with Machine Learning," *AIAA Journal*, Vol. 59, No. 8, 2021, pp. 2820–2847. https://doi.org/10.2514/1.j060131

[21] Li, J., Du, X., and Martins, J. R. R. A., "Machine Learning in Aerodynamic Shape Optimization," *Progress in Aerospace Sciences* (submitted for publication).

[22] Li, J., Bouhlel, M. A., and Martins, J. R. R. A., "Data-Based Approach for Fast Airfoil Analysis and Optimization," *AIAA Journal*, Vol. 57, No. 2, 2019, pp. 581–596. https://doi.org/10.2514/1.J057129

[23] Bouhlel, M. A., He, S., and Martins, J. R. R. A., "Scalable Gradient-Enhanced Artificial Neural Networks for Airfoil Shape Design in the Subsonic and Transonic Regimes," *Structural and Multidisciplinary Optimization*, Vol. 61, March 2020, pp. 1363–1376. https://doi.org/10.1007/s00158-020-02488-5

[24] Li, J., and Zhang, M., "Data-Based Approach for Wing Shape Design Optimization," *Aerospace Science and Technology*, Vol. 112, May 2021, Paper 106639. https://doi.org/10.1016/j.ast.2021.106639

[25] Du, X., He, P., and Martins, J. R. R. A., "Rapid Airfoil Design Optimization via Neural Networks-Based Parameterization and Surrogate Modeling," *Aerospace Science and Technology*, Vol. 113, June 2021, Paper 106701. https://doi.org/10.1016/j.ast.2021.106701

[26] Li, J., and Zhang, M., "Adjoint-Free Aerodynamic Shape Optimization of the Common Research Model Wing," *AIAA Journal*, Vol. 59, No. 6, 2021, pp. 1990–2000. https://doi.org/10.2514/1.J059921

[27] Li, J., and Zhang, M., "On Deep-Learning-Based Geometric Filtering in Aerodynamic Shape Optimization," *Aerospace Science and Technology*, Vol. 112, May 2021, Paper 106603. https://doi.org/10.1016/j.ast.2021.106603

[28] Li, J., "Machine-Learning-Based Compact Geometric Design Space for Efficient Aerodynamic Shape Optimization," 2021. https://doi.org/10.13140/RG.2.2.14934.37447

[29] Vassberg, J. C., Dehaan, M. A., Rivers, S. M., and Wahls, R. A., "Development of a Common Research Model for Applied CFD Validation Studies," *26th AIAA Applied Aerodynamics Conference*, AIAA Paper 2008-6919, Aug. 2008. https://doi.org/10.2514/6.2008-6919

[30] Schmitt, V., and Charpin, F., "Pressure Distributions on the ONERA-M6-Wing at Transonic Mach Numbers," AGARD AR-138, 1979.

[31] Lyu, Z., and Martins, J. R. R. A., "Aerodynamic Design Optimization Studies of a Blended-Wing-Body Aircraft," *Journal of Aircraft*, Vol. 51, No. 5, 2014, pp. 1604–1617. https://doi.org/10.2514/1.C032491

[32] Liebeck, R. H., "Design of the Blended Wing Body Subsonic Transport," *Journal of Aircraft*, Vol. 41, No. 1, 2004, pp. 10–25. https://doi.org/10.2514/1.9084

[33] Bérard, A., and Isikveren, A. T., "Conceptual Design Prediction of the Buffet Envelope of Transport Aircraft," *Journal of Aircraft*, Vol. 46, No. 5, 2009, pp. 1593–1606. https://doi.org/10.2514/1.41367

[34] Paladini, E., Dandois, J., Sipp, D., and Robinet, J.-C., "Analysis and Comparison of Transonic Buffet Phenomenon over Several Three-Dimensional Wings," *AIAA Journal*, Vol. 57, No. 1, 2019, pp. 379–396. https://doi.org/10.2514/1.J056473

[35] Rumsey, C. L., Allison, D. O., Biedron, R. T., Buning, P. G., Gainer, T. G., Morrison, J. H., Rivers, S. M., Mysko, S. J., and Witkowski, D. P., "CFD Sensitivity Analysis of a Modern Civil Transport Near Buffet-Onset Conditions," NASA TM-2001-211263, 2001.

[36] Mader, C. A., Kenway, G. K. W., Yildirim, A., and Martins, J. R. R. A., "ADflow: An Open-Source Computational Fluid Dynamics Solver for Aerodynamic and Multidisciplinary Optimization," *Journal of Aerospace Information Systems*, Vol. 17, No. 9, 2020, pp. 508–527. https://doi.org/10.2514/1.I010796

[37] Munguía, B. C., Mukhopadhaya, J., and Alonso, J. J., "Shock-Induced Separation Suppression Using CFD-Based Active Flow Control Optimization," *AIAA SciTech 2019 Forum*, AIAA Paper 2019-0695, Jan. 2019. https://doi.org/10.2514/6.2019-0695

[38] McDevitt, J. B., Levy, L. L., and Deiwert, G. S., "Transonic Flow About a Thick Circular-Arc Airfoil," *AIAA Journal*, Vol. 14, No. 5, 1976, pp. 606–613. https://doi.org/10.2514/3.61402

[39] Steimle, P. C., Karhoff, D.-C., and Schröder, W., "Unsteady Transonic Flow over a Transport-Type Swept Wing," *AIAA Journal*, Vol. 50, No. 2, 2012, pp. 399–415. https://doi.org/10.2514/1.J051187

[40] Lee, B. H. K., "Self-Sustained Shock Oscillations on Airfoils at Transonic Speeds," *Progress in Aerospace Sciences*, Vol. 37, No. 2, 2001, pp. 147–196. https://doi.org/10.1016/S0376-0421(01)00003-3

[41] Iovnovich, M., and Raveh, D. E., "Numerical Study of Shock Buffet on Three-Dimensional Wings," *AIAA Journal*, Vol. 53, No. 2, 2015, pp. 449–463. https://doi.org/10.2514/1.J053201

[42] Li, J., Zhang, M., Martins, J. R. R. A., and Shu, C., "Efficient Aerodynamic Shape Optimization with Deep-Learning-Based Filtering," *AIAA*

Journal, Vol. 58, No. 10, 2020, pp. 4243–4259.
https://doi.org/10.2514/1.J059254

[43] Perez, R. E., Jansen, P. W., and Martins, J. R. R. A., "pyOpt: A Python-Based Object-Oriented Framework for Nonlinear Constrained Optimization," *Structural and Multidisciplinary Optimization*, Vol. 45, No. 1, 2012, pp. 101–118.
https://doi.org/10.1007/s00158-011-0666-3

[44] Wu, N., Kenway, G., Mader, C. A., Jasa, J., and Martins, J. R. R. A., "pyOptSparse: A Python Framework for Large-Scale Constrained Nonlinear Optimization of Sparse Systems," *Journal of Open Source Software*, Vol. 5, No. 54, 2020, p. 2564.
https://doi.org/10.21105/joss.02564

[45] Kenway, G. K., Kennedy, G. J., and Martins, J. R. R. A., "A CAD-Free Approach to High-Fidelity Aerostructural Optimization," *Proceedings of the 13th AIAA/ISSMO Multidisciplinary Analysis Optimization Conference*, AIAA Paper 2010-9231, Sept. 2010.
https://doi.org/10.2514/6.2010-9231

[46] Lambe, A. B., and Martins, J. R. R. A., "Extensions to the Design Structure Matrix for the Description of Multidisciplinary Design, Analysis, and Optimization Processes," *Structural and Multidisciplinary Optimization*, Vol. 46, Jan. 2012, pp. 273–284.
https://doi.org/10.1007/s00158-012-0763-y

[47] Yildirim, A., Kenway, G. K. W., Mader, C. A., and Martins, J. R. R. A., "A Jacobian-Free Approximate Newton–Krylov Startup Strategy for RANS Simulations," *Journal of Computational Physics*, Vol. 397, Nov. 2019, Paper 108741.
https://doi.org/10.1016/j.jcp.2019.06.018

[48] Bhatnagar, S., Afshar, Y., Pan, S., Duraisamy, K., and Kaushik, S., "Prediction of Aerodynamic Flow Fields Using Convolutional Neural Networks," *Computational Mechanics*, Vol. 64, No. 2, 2019, pp. 525–545.
https://doi.org/10.1007/s00466-019-01740-0

[49] Fukami, K., Nakamura, T., and Fukagata, K., "Convolutional Neural Network Based Hierarchical Autoencoder for Nonlinear Mode Decomposition of Fluid Field Data," *Physics of Fluids*, Vol. 32, No. 9, 2020, Paper 095110.
https://doi.org/10.1063/5.0020721

[50] Zhang, Y., Sung, W. J., and Mavris, D. N., "Application of Convolutional Neural Network to Predict Airfoil Lift Coefficient," *2018 AIAA/ASCE/AHS/ASC Structures, Structural Dynamics, and Materials Conference*, AIAA Paper 2018-1903, Jan. 2018.
https://doi.org/10.2514/6.2018-1903

[51] Chen, H., He, L., Qian, W., and Wang, S., "Multiple Aerodynamic Coefficient Prediction of Airfoils Using a Convolutional Neural Network," *Symmetry*, Vol. 12, No. 4, 2020, p. 544.
https://doi.org/10.3390/sym12040544

[52] Masoudnia, S., and Ebrahimpour, R., "Mixture of Experts: A Literature Survey," *Artificial Intelligence Review*, Vol. 42, No. 2, 2014, pp. 275–293.
https://doi.org/10.1007/s10462-012-9338-y

[53] Liem, R. P., Mader, C. A., and Martins, J. R. R. A., "Surrogate Models and Mixtures of Experts in Aerodynamic Performance Prediction for Aircraft Mission Analysis," *Aerospace Science and Technology*, Vol. 43, June 2015, pp. 126–151.
https://doi.org/10.1016/j.ast.2015.02.019

[54] Lyu, Z., Kenway, G. K. W., and Martins, J. R. R. A., "Aerodynamic Shape Optimization Investigations of the Common Research Model Wing Benchmark," *AIAA Journal*, Vol. 53, No. 4, 2015, pp. 968–985.
https://doi.org/10.2514/1.J053318

[55] Martins, J. R. R. A., and Ning, A., *Engineering Design Optimization*, Cambridge Univ. Press, Cambridge, England, U.K., 2022, pp. 146–147, https://mdobook.github.io [retrieved 10 May 2022].
https://doi.org/10.1017/9781108980647

[56] Kenway, G. K. W., Mader, C. A., He, P., and Martins, J. R. R. A., "Effective Adjoint Approaches for Computational Fluid Dynamics," *Progress in Aerospace Sciences*, Vol. 110, Oct. 2019, Paper 100542.
https://doi.org/10.1016/j.paerosci.2019.05.002

K. Taira
Associate Editor